JOURNAL OF COMPUTATIONAL PHYSICS 60, 167–186 (1985)

Numerical Schemes for a Model for Nonlinear Dispersive Waves

J. L. BONA

Department of Mathematics, University of Chicago, Chicago, Illinois 60637

W. G. PRITCHARD

Fluid Mechanics Research Institute, University of Essex, Colchester, Essex CO4 3SQ, United Kingdom

AND

L. R. SCOTT

Department of Mathematics, University of Michigan, Ann Arbor, Michigan 48109

Received October 19, 1983; revised October 22, 1984

A description is given of a number of numerical schemes to solve an evolution equation that arises when modelling the propagation of water waves in a channel. The discussion also includes the results of numerical experiments made with each of the schemes. It is suggested, on the basis of these experiments, that one of the schemes may have (discrete) solitary-wave solutions.

1. INTRODUCTION

In this paper we examine some numerical schemes for the initial-value problem for the real-valued function $u(x, t)$ given by

$$u_t + u_x + \beta u u_x - \gamma^{-2} u_{xxt} = 0, \qquad x \in \mathbb{R},\ t > 0, \tag{P1}$$

$$u(x, 0) = g(x), \tag{P2}$$

where $\beta \geqslant 0$ and $\gamma > 0$ are constants, and g is a given function comprising the initial datum for the differential equation. This problem, which arises in the theory of water waves, has been studied in recent years by several workers: Peregrine [17] examined its possible relevance to the temporal development of undular bores; a

0021-9991/85 $3.00

mathematical theory for the problem was developed by Benjamin, Bona, and Mahony [5]; and, more recently, the present authors [9] have made a detailed comparison of the model with the outcome of some laboratory experiments. The problem (P) is closely associated with the initial-value problem for the Korteweg–de Vries equation

$$u_t + u_x + \beta u u_x + \gamma^{-2} u_{xxx} = 0, \tag{1.1}$$

in that both equations have been advocated as models for the same physical phenomena (e.g., see Benjamin *et al.* [5]). Indeed, when the initial datum g is restricted to conform to that arising in many physical applications, it can be shown (see Bona, Pritchard, and Scott [10]) that the two equations yield essentially the same solution over a non-trivial time scale. The latter work also points out some other qualitative similarities between the solutions of the two problems over longer time scales.

Several numerical studies of (P), or closely associated problems, have been reported: e.g., see Peregrine [17], Wahlbin [21], Eilbeck and McGuire [12, 13], Santarelli [18], Courtenay Lewis and Tjon [11], Alexander and Morris [3], Bona *et al.* [8, 9]. Abdulloev *et al.* [1] describe the results of some interesting computations for (P), but no details are given of the methods employed. Most of these studies present the results of formal calculations, except for the work of Wahlbin, in which an analysis is given of a Galerkin method for a (spatially) periodic version of (P), and that of [9], in which an analysis is given of a finite-difference method for an initial- and boundary-value version of (P). Both of the latter studies also showed that a specific implementation of the methods displayed the expected convergence properties when the mesh was refined.

While developing the numerical method used in [9] we also developed and tested a number of finite-difference schemes for (P), and the purpose of the present paper is to describe some of the comparisons that were made between these various schemes. A description is given in Section 2 of the methods studied, consisting of a second-order method and a number of fourth-order schemes. The discussion also indicates how efficient schemes having arbitrary order accuracy can be generated. In Section 3 a discussion is given of the numerical experiments, including standard convergence studies along with a number of more subtle, subsidiary experiments.

The main numerical experiments described below are related to special solutions to (P) known as solitary waves, which occur in the case $\beta > 0$. This one-parameter family of solutions represents single-crested waves of elevation and is given by

$$u(x, t) = U \operatorname{sech}^2\{\alpha[(x - x_0) - (1 + \tfrac{1}{3}\beta U)t]\}, \tag{1.2}$$

for $U > 0$ and $\alpha = [\frac{1}{12}\beta\gamma^2 U(1 + \frac{1}{3}\beta U)^{-1}]^{1/2}$, corresponding to the initial datum

$$g(x) = U \operatorname{sech}^2[\alpha(x - x_0)]. \tag{1.3}$$

The arbitrary parameter x_0 gives the location of the point of maximum amplitude of the solitary wave at time $t = 0$. These solitary waves propagate without change of form at the steady speed $(1 + \frac{1}{3}\beta U)$, determined by their maximum amplitude U. (Note that if $U < -3/\beta$, (1.2) also defines a real-valued travelling-wave solution of depression, whose amplitude, however, excludes it from the range of physical interest.)

An especially interesting feature to emerge from our numerical experiments is that one of the schemes under study appeared to have a discrete solitary-wave solution.

2. The Numerical Schemes

In this section a description is given of the various schemes that have been studied. First we shall describe several semidiscrete, spatial approximations to the solution to (P) and then go on to describe the temporal approximations that have been used. As indicated in the Introduction, Benjamin *et al.* [5] showed that (P) is a well-posed problem. In particular, they showed that if g and its first few derivatives are continuous and bounded, then corresponding to g there is a unique bounded solution u of (P). This solution is infinitely differentiable with respect to the temporal variable t and is as smooth in the spatial variable x as the datum g. For such bounded solutions u they also derived an integral representation, namely,

$$u_t(x, t) = \int_{-\infty}^{\infty} K(x, y)(u + \tfrac{1}{2}\beta u^2)(y, t)\, dy, \tag{2.1}$$

where $K(x, y) := \frac{1}{2}\gamma^2 \operatorname{sgn}(x - y)\, e^{-\gamma|x-y|}$. This representation has been used to generate the spatial discretizations described here. The ideas outlined below are closely related to the work described in [9], to which paper repeated reference will be made for some of the technical issues that arise.

2.1. *Spatial Discretizations*

2.1.1. *The GEM Scheme*

The spatial discretizations were effected first by truncating the infinite interval of integration to a finite interval $[X_1, X_2]$ and then by taking quadrature approximations of the integrals

$$\int_{X_1}^{x} K(x, y)(u + \tfrac{1}{2}\beta u^2)(y, t)\, dy \qquad \text{and} \qquad \int_{x}^{X_2} K(x, y)(u + \tfrac{1}{2}\beta u^2)(y, t)\, dy. \tag{2.2}$$

Justification for the truncation of the infinite interval can be given using arguments of the kind described in [9]. Note that K is smooth except for a jump discontinuity on the diagonal $y = x$ and so, by splitting the interval of integration at x, the smoothness of the integrand on each of the subinterivals is determined entirely by

the smoothness of the initial datum g (cf. (2.1)). The quadrature approximation of the integrals used here is the Euler–Maclaurin formula truncated at fourth order, namely the trapezoidal rule on a uniform mesh with one derivative correction at each of the end points of the ranges of integration. When these derivative corrections fall upon the unknown $(u+\frac{1}{2}\beta u^2)$ they are approximated by a centered, second difference. This discretization gives a quadrature rule similar to the one derived by Gregory (cf. Goldstine [14]) prior to the work of Euler and Maclaurin, the only difference being that here derivatives of K have been found exactly. A further simplification can be made, as indicated in [9], by ignoring certain small terms arising at the extremities X_1 and X_2 of the interval of integration.

These approximations lead to a system of ordinary differential equations for functions $u_i(t)$, where u_i approximates u at the ith quadrature point (i.e., $u_i(t) \sim u(i\,\Delta x, t)$). Here $i = N_1, N_1+1, \ldots, N_2$, with $X_1 := N_1 \Delta x$, $X_2 := N_2 \Delta x$, and Δx denotes the mesh size. These equations comprise a semidiscrete approximation to (2.1), taking the form

$$\dot{u}_i(t) = F_i((\mathbf{u} + \tfrac{1}{2}\beta \mathbf{u} \circ \mathbf{u})(t)), \qquad i = N_1, \ldots, N_2, \tag{2.3}$$

where $\mathbf{u} = (u_{N_1}, \ldots, u_{N_2})$, the symbol $\mathbf{u} \circ \mathbf{u}$ is defined by

$$(\mathbf{u} \circ \mathbf{u})_i := u_i^2, \tag{2.4}$$

and $F_i(\mathbf{v}) = F_i(v_{N_1}, \ldots, v_{N_2})$ is given by

$$F_i(\mathbf{v}) := \Delta x \left\{ \sum_{j=N_1}^{N_2} K(i\,\Delta x, j\,\Delta x)\, v_j - \frac{1}{24}\gamma^2 (v_{i+1} - v_{i-1}) \right\}, \tag{2.5}$$

with the understanding that $K(x, x) = 0$ for all x, and $v_{N_1-1} = v_{N_2+1} = 0$ whenever these expressions appear. More complete details of the derivation of these formulae can be found in [9]. We shall refer to the spatial discretization (2.3)–(2.5), as well as the simplification to be described below, as the Gregory–Euler–Maclaurin (GEM) scheme.

As it stands the method (2.3)–(2.5) involves a discrete convolution to calculate $\mathbf{F} = (F_{N_1}, \ldots, F_{N_2})$ and is therefore not a very efficient procedure. However, this may be overcome in the following way. Define a second-difference operator $\mathbf{D}^2$ such that

$$(\mathbf{D}^2 \mathbf{v})_i := v_i - (v_{i+1} - 2v_i + v_{i-1})/(e^{\gamma \Delta x} - 2 + e^{-\gamma \Delta x}), \tag{2.6}$$

which we write in the form

$$a v_i + b(v_{i+1} + v_{i-1}),$$

so that $a = 1 - 2b$ and $-b^{-1} = (2 \sinh(\frac{1}{2}\gamma\, \Delta x))^2$ $(= (\gamma\, \Delta x)^2 + O(\gamma\, \Delta x)^4)$. We want to apply $\mathbf{D}^2$ to the convolution term of (2.5), and it is therefore convenient to split $\mathbf{F}$ into two parts, namely,

$$F_i(\mathbf{v}) = F_i^1(\mathbf{v}) + F_i^2(\mathbf{v}),$$

where F_i^1 is the convolution term and $F_i^2(\mathbf{v}) := -\frac{1}{24}\gamma^2\,\Delta x(v_{i+1}-v_{i-1})$. Then, for $N_1 < i < N_2$, a straightforward calculation gives

$$(\mathbf{D}^2\mathbf{F}^1(\mathbf{v}))_i = \tfrac{1}{2}b\gamma^2\,\Delta x(v_{i+1}-v_{i-1}) = -12bF_i^2(\mathbf{v}). \tag{2.7}$$

If again we ignore terms involving points outside the interval $[X_1, X_2]$, an approximation to $\mathbf{F}^1$ (which is appropriate if $\mathbf{v}$ is suitably small near X_1 and X_2, as obtains here) is given by the solution $\mathbf{f}(\mathbf{v})$ to the tridiagonal system of equations

$$\mathbf{A}\mathbf{f} = -12b\mathbf{F}^2(\mathbf{v}), \tag{2.8}$$

where

$$\mathbf{A} = \begin{bmatrix} a & b & & & & \\ b & a & b & & & \\ & \ddots & \ddots & \ddots & & \\ & & b & a & b & \\ & & & b & a & \end{bmatrix}.$$

Thus, it is more efficient computationally to use the semidiscrete scheme

$$\begin{aligned} \dot{\mathbf{u}}(t) &= \tilde{\mathbf{F}}((\mathbf{u} + \tfrac{1}{2}\beta\mathbf{u}\circ\mathbf{u})(t)), \\ u_i(0) &= g(i\,\Delta x), \qquad i = N_1, \ldots, N_2, \end{aligned} \tag{2.9(GEM)}$$

where $\tilde{\mathbf{F}} = \mathbf{f} + \mathbf{F}^2$, and for which $\tilde{\mathbf{F}}$ can be calculated in $O(N_2 - N_1)$ operations by solving the tridiagonal system (2.8). Using the same methods as those described in [9], it can be shown that (2.9) has an accuracy of

$$O(\Delta x^4 - e^{-r(X_2 - X_1)}), \tag{2.10}$$

where r is a positive constant.

Although (2.9) does not appear, superficially, to be a standard discretization it can, nevertheless, be viewed as a finite-difference approximation to (2.1) (or P1) written in the form

$$(1 - \gamma^{-2}\partial_x^2)\,u_t = -\partial_x(u + \tfrac{1}{2}\beta u^2). \tag{P1, \textit{bis}}$$

To see this define difference operators $\mathbf{D}^1$ and $\mathbf{D}_0^2$ by

$$\begin{aligned} (\mathbf{D}^1\mathbf{v})_i &:= (v_{i+1} - v_{i-1})/2\Delta x, \\ (\mathbf{D}_0^2\mathbf{v})_i &:= -(v_{i-1} - 2v_i + v_{i+1})/\Delta x^2, \end{aligned} \tag{2.11}$$

and a parameter κ by

$$\kappa := -b\,\Delta x^2 = (\Delta x/2\sinh(\tfrac{1}{2}\gamma\,\Delta x))^2. \tag{2.12}$$

Then, after multiplying the (GEM) scheme by $\mathbf{D}^2 := \mathbf{I} + \kappa \mathbf{D}_0^2$, and using the definition (2.8) of $\mathbf{f}$, it follows that

$$(I + \kappa D_0^2)\,\dot{\mathbf{u}} = -\gamma^2[(\kappa + \tfrac{1}{12}\Delta x^2)I + \tfrac{1}{12}\kappa\,\Delta x^2 D_0^2]\,D^1\mathbf{v}, \qquad (2.13)(\text{GEM})$$

where

$$\begin{aligned} v_i &:= u_i + \tfrac{1}{2}\beta u_i^2, \qquad N_1 \leqslant i \leqslant N_2, \\ &:= 0, \qquad\qquad \text{otherwise}, \end{aligned} \qquad (2.14)$$

and $u_i := (\mathbf{u})_i$, $N_i \leqslant i \leqslant N_2$, $u_i := 0$ otherwise.

Note that

$$\kappa = \gamma^{-2}[1 - \tfrac{1}{12}(\gamma\,\Delta x)^2 + O((\gamma\,\Delta x)^4)], \qquad (2.15)$$

which, together with (2.13), can be used to generate other discrete methods for (P1).

2.1.2. *A Second-Order Method*

At second order the (GEM) scheme agrees with the second-order centered-difference approximation to (P1), namely,

$$(\mathbf{I} + \gamma^{-2}\mathbf{D}_0^2)\,\dot{\mathbf{u}} = -\mathbf{D}^1\mathbf{v}, \qquad (2.16)(\text{CD})$$

with $\mathbf{v}$ defined as in (2.14).

This kind of spatial differencing has often been used (e.g., see Eilbeck and McGuire [12]), though sometimes the nonlinear term is not cast in the "conservative" form used here.

2.1.3. *Another Fourth-Order Method*

Keeping terms in (2.13) only to fourth order yields an approximation to (P1) of Störmer–Numerov type (cf. Stoer and Bulirsch [20]), namely,

$$(\mathbf{I} + \gamma^{-2}(1 - \tfrac{1}{12}(\gamma\,\Delta x)^2)\,\mathbf{D}_0^2)\,\dot{\mathbf{u}} = -(I + \tfrac{1}{12}\Delta x^2\mathbf{D}_0^2)\,\mathbf{D}^1\mathbf{v}, \qquad (2.17)(\text{SN})$$

and again $\mathbf{v}$ is defined as in (2.14).

As with the (GEM) scheme, this method can be shown to satisfy the error bound (2.10), some specific tests of which are described below.

2.1.4. *Remarks*

(i) Although the (GEM) scheme ((2.9) or (2.13)–(2.14)) has only fourth-order spatial accuracy, schemes of arbitrary-order accuracy can be derived in a similar way by retaining the required number of terms in the Euler–Maclaurin formula (with the appropriate derivative corrections being replaced by differences). For these higher-order schemes the system of equations corresponding to (2.8) is not altered, the only change in the scheme being that $\tilde{\mathbf{F}}$ is of the form $\tilde{\mathbf{F}} = \mathbf{f} + \tilde{\mathbf{F}}^2$, where $\mathbf{F}^2$ incorporates the higher-order derivative corrections; the original $\mathbf{F}^2$,

however, remains on the right-hand side of (2.8). This occurs because the difference operator $\mathbf{D}^2$ $(=\mathbf{I}+\kappa\mathbf{D}_0^2)$ is an infinite-order approximation to $(1-\gamma^{-2}\partial_x^2)$, in the sense that

$$\mathbf{D}^2(1-\gamma^{-2}\partial_x^2)^{-1}\partial_x\phi=\kappa\mathbf{D}^1\phi,$$

for all sufficiently regular functions ϕ. Thus the term $\mathbf{f}$ in the definition of $\tilde{\mathbf{F}}$ is infinite-order accurate, and it remains only to determine $\tilde{\mathbf{F}}^2$ to the desired accuracy.

(ii) It is more efficient to compute the (GEM) scheme in the form (2.8)–(2.9) than in the form (2.13): with the fourth-order scheme, for example, the latter arrangement requires the calculation of a penta-diagonal approximation to ∂_x, whereas the former involves only $\mathbf{D}^1$. In general, one could envisage a variable-order method where $\tilde{\mathbf{F}}^2$ is calculated to different orders of accuracy in different parts of the domain (depending, say, on some local estimation of the spatial errors).

(iii) The generalisation of the (GEM) scheme to obtain higher-order methods may appear somewhat academic, but the use of the fourth-order scheme in [9] (in modelling a laboratory experiment) placed a considerable burden on the data sampling to ensure the desired accuracy of the numerical solutions. Similarly, in another study concerning the interaction properties of two solitary-wave solutions of the family (1.2) (see Bona *et al.* [8]), the implementation of a more accurate scheme would have been beneficial. At the outset of each of these projects the fourth-order scheme seemed to be more than adequate but, in retrospect, we should have considered more seriously the relative efficiency of the higher-order schemes.

(iv) The above methods can readily be adapted to solve (P1) posed on some fixed interval $[X_1, X_2]$, subject to the initial condition that $u(x,0)=g(x)$ for $X_1\leqslant x\leqslant X_2$ and the boundary conditions $u(X_i,t)=h_i(t)$ for $t\geqslant 0$, $i=1, 2$, where g, h_1 and h_2 are given functions. (Theory relating to this initial- and two-point boundary-value problem has been provided by Showalter [19] and Bona and Dougalis [7]. In case $X_1=-\infty$ or $X_2=+\infty$, the condition $u(X_i,t)=h_i(t)$ may be replaced by a growth condition, as in Bona and Bryant [6].) These methods may also be used to handle the periodic initial-value problem in which the initial datum g and the solution u are both required to be periodic in x with a given period. We have implemented the GEM scheme for some of these problems.

2.2. *Temporal Discretization*

All the spatial discretizations of (P) described above lead to a system of ordinary-differential equations of the form

$$\begin{aligned}&\dot{\mathbf{u}}(t)=\mathscr{F}(\mathbf{u}(t)), \qquad t\geqslant 0,\\ &\mathbf{u}(0)=\mathbf{u}^0,\end{aligned} \tag{2.18}$$

where, for example, $u_i^0=g(i\,\Delta x)$ for $N_1\leqslant i\leqslant N_2$. Moreover, the function $\mathscr{F}$ remains suitably bounded as $\Delta x\to 0$, so that the problem (2.18) is not in any way stiff for

small values of Δx. An indication of why this is so is given by a von Neumann-type stability analysis of a linearized version of the problem with periodic boundary conditions. Thus, in (2.14), set $v_i = Uu_i$ for all i, where U is a constant, and consider the above discretizations for the initial-value problem for the appropriate modification to (P), and with 2π-periodic data and corresponding periodic boundary conditions in space. Then, for all three of the above spatial discretizations, the resulting $\mathbf{F}$ has eigenvalues μ_k of the form

$$\mu_k = iU\gamma\lambda_k,$$

where $0 \leqslant k < 2\pi/\Delta x$ and, for each k, λ_k is real with $|\lambda_k| \leqslant C$, where C remains bounded as Δx approaches zero. In particular, we may take

$$\begin{aligned} C &= \tfrac{1}{2}, && \text{for CD(2.16),} \\ &= \tfrac{1}{2} + \tfrac{1}{12}\gamma\,\Delta x, && \text{for GEM(2.13)–(2.14), and} \\ &= (1 - \tfrac{1}{12}(\gamma\,\Delta x)^2)^{-1/2}, && \text{for SN(2.17).} \end{aligned}$$

Note that, for the (SN) scheme, we must have $\Delta x < 144\gamma^{-1}$ in order that the multiple of $\mathbf{D}_0^2$ on the left-hand side of (2.17) be positive. For the full nonlinear problem the precise boundedness conditions satisfied by $\mathscr{F}$ are given in [9]. It follows that any of a variety of methods for integrating ordinary differential equations can be used to discretize (2.18). This observation is generally valid for the class of Sobolev equations, of which (P1) is a prototype (cf. Arnold, Douglas, and Thomée [4]).

For the second-order scheme (2.16) it is natural to consider a second-order temporal discretization and, since stiffness is not a problem, an explicit method can be used. We have therefore chosen the so-called "leap-frog" scheme

$$\mathbf{u}^{n+1} = \mathbf{u}^{n-1} + 2\Delta t\mathscr{F}(\mathbf{u}^n), \qquad n \geqslant 1. \tag{2.19(LF)}$$

The "starting value" $\mathbf{u}^1$ was obtained from a step using the Runge–Kutta scheme described below. (In fact, for the numerical experiments to be reported in Section 3, three steps of (RK) were used initially so that (LF) was used only for $n \geqslant 3$.) The discretization (2.16), (2.19) of (P), the (CD–LF) scheme, has an error bound of the form

$$O(\Delta x^2 + \Delta t^2 + e^{-r(X_2 - X_1)}), \tag{2.20}$$

where r is a positive constant.

For the fourth-order schemes (GEM) (2.8, 2.9) and (SN) we have used the following fourth-order Runge–Kutta method, for $n \geqslant 0$:

$$\begin{aligned} \mathbf{w}^1 &= \mathbf{u}^n + \tfrac{1}{2}\Delta t\mathscr{F}(\mathbf{u}^n), \\ \mathbf{w}^2 &= \mathbf{u}^n + \tfrac{1}{2}\Delta t\mathscr{F}(\mathbf{w}^1), \\ \mathbf{w}^3 &= \mathbf{u}^n + \Delta t\mathscr{F}(\mathbf{w}^2), \\ \mathbf{u}^{n+1} &= \mathbf{u}^n + \tfrac{1}{6}\Delta t[2\mathscr{F}(\mathbf{w}^1) + 2\mathscr{F}(\mathbf{w}^2) + \mathscr{F}(\mathbf{u}^n) + \mathscr{F}(\mathbf{w}^3)]. \end{aligned} \tag{2.21(RK)}$$

Once several steps of (RK) have been calculated it could prove more efficient to switch to a multi-step scheme. We have, therefore, also considered the following prediction-correction scheme, for $n \geq 3$:

$$\begin{aligned} \tilde{\mathbf{u}}^{n+1} &= \mathbf{u}^n + \tfrac{1}{24}\Delta t[55\mathscr{F}^n - 59\mathscr{F}^{n-1} + 39\mathscr{F}^{n-2} - 9\mathscr{F}^{n-3}], \\ \mathbf{u}^{n+1} &= \mathbf{u}^n + \tfrac{1}{720}\Delta t[251\mathscr{F}(\tilde{\mathbf{u}}^{n+1}) + 646\mathscr{F}^n \\ &\qquad - 264\mathscr{F}^{n-1} + 106\mathscr{F}^{n-2} - 19\mathscr{F}^{n-3}], \end{aligned} \tag{2.22(MS)}$$

where $\mathscr{F}^j$ denotes $\mathscr{F}(\mathbf{u}^j)$ and $\mathbf{u}^1$, $\mathbf{u}^2$, and $\mathbf{u}^3$ are calculated by (2.21). (Note that this prediction–correction scheme is used in the so-called PECE mode, as described by Lambert [16]. The prediction step employs the fourth-order Adams–Bashforth formula while the correction step is made via the fifth-order Adams-Moulton method. This results in a temporal discretization that has fifth-order accuracy.)

All four possible combinations of the spatial discretizations (GEM) or (SN), coupled with the temporal discretizations (RK) or (MS), provide a fully discrete approximation to (P) satisfying the error bound

$$O(\Delta x^4 + \Delta t^p + e^{-r(X_2 - X_1)}), \tag{2.23}$$

where p is four for the (RK) scheme and five for the (MS) scheme, and r is a positive constant.

The (GEM) spatial discretization, coupled with the standard fourth-order Adams–Bashforth–Moulton prediction–correction scheme (e.g., see Lambert [16]), was used in [9] to solve (P1) posed with initial and boundary conditions.

3. Numerical Experiments

3.1. *Preliminary Definitions*

In this section a description is given of some numerical experiments made with our implementations of the above methods. All the experiments to be described relate to initial data $g(x)$ given by (1.3). This function is associated with the family (1.2) of exact solutions to the problem (P) and therefore provides a convenient means of checking the convergence properties of the various schemes. It has, in addition, enabled us to make a number of other, more refined, studies of the properties of the numerical solutions.

It is standard practice to determine empirically the convergence of a scheme to test both its theoretical basis and the correctness of its implementation. Fairly detailed studies of this kind have been made for the methods under consideration, but we give here only a sample of the results that have been obtained. All the experiments to be described were made with $\beta = 1.5$ and $\gamma^2 = 6$, identifications which henceforth will be assigned without further reference. These values relate to the aforementioned physical problem of water waves propagating in a uniform

channel. (We have, however, carried out similar tests with other values of β and γ.) Thus, the quantity α appearing in (1.2) is given by $\alpha = [3U/4(1+\frac{1}{2}U)]^{1/2}$, and the solitary wave of amplitude U has speed $c := (1+\frac{1}{2}U)$.

The truncation of the infinite interval described in Section 2 was usually effected, at $t=0$, by choosing X_1 and X_2 such that

$$g(X_i)/U = \varepsilon, \qquad i = 1, 2. \tag{3.1}$$

Here ε was chosen empirically so that the truncation had negligible influence on the results. At each time step (or after a certain specified number of time steps) the right-hand boundary was moved outwards (i.e., X_2 was increased) so that its distance from the "crest" of the solitary wave did not, on average, decrease with time. Whenever such an expansion of the domain was made the vector $\mathbf{u}$ was extended by zero on its undefined components. In certain experiments it was also possible to move the left-hand boundary X_1 to the right without influencing appreciably the experiment in question. (In such cases, the vector $\mathbf{u}$ was simply truncated.) The changes in X_1 and X_2 were made automatically by the code, as follows. After each M time steps the values of X_1 and X_2 were moved a distance $C_i \Delta t M$, corresponding to speeds C_1 and C_2. A typical value for M was 25 and C_1 and C_2 were chosen appropriately for specific computations. In particular $C_1 \leqslant 1 + \frac{1}{2}U \leqslant C_2$. We were conservative about the positioning of the endpoints of the domain but, even so, in some of the experiments with very fine meshes the errors generated by the numerical scheme were so small that the positioning of the boundaries (at $t=0$) gave rise to a nonnegligible additional error. However, this additional contribution was never more than 5% of the total error. We shall not, therefore, report the values of $X_1(t)$ and $X_2(t)$, but give only their values at $t=0$. These will be stated implicitly by quoting either x_0 (cf. (1.3)), in which case $X_1 = 0$ and $X_2 = 2x_0$, or by quoting the value of ε in (3.1).

To describe the convergence studies it is convenient to introduce some definitions. Let a solution to the discrete problem at time $t = j\Delta t$, where j is a positive integer, be denoted by $\boldsymbol{\eta}(t) = (..., \eta_i(t), ...)$, $N_1(t) \leqslant i \leqslant N_2(t)$, and let the exact solution (1.2) be denoted by $u(x, t)$. Define a relative difference E between the two functions by

$$E(t) := \left\{ \sum_{i=N_1}^{N_2} [u(i\Delta x, t) - \eta_i(t)]^2 \Big/ \sum_{i=N_1}^{N_2} [u(i\Delta x, t)]^2 \right\}^{1/2}. \tag{3.2}$$

Another functional of interest in this problem is the difference between the *amplitude* η_m of the discrete solution and that of the solution of the continuous problem, a difference we shall refer to as the *height error* $H(t)$. This quantity is defined in the following way. Find $\max\{\eta_i(t): N_1(t) \leqslant i \leqslant N_2(t)\}$; let p be the value of i at which the maximum is achieved. (If there is more than one such i, let p be the smallest of these.) Then interpolate the function values $\eta_i(t)$ by a quartic polynomial $Q(x)$ at the points $x = i\Delta x$, for $i = p + k$ with $|k| \leqslant 2$ (i.e., at the five

points centered about the maximum of η). Now determine the maximum value of Q using Newton's method, starting the iteration at $x = p\,\Delta x$. (This procedure was successful in all cases.) Denote this maximum by η_m. Then, finally, define the height error to be

$$H(t) := U - \eta_m(t). \tag{3.3}$$

The value of x for which Q achieves its maximum, say x_m, provides the possibility of determining a phase error at each t for the discrete solution and, by taking differences, of obtaining an average speed for the wave crest in the discrete solution. This speed can then be compared with the speed c of the solitary-wave solution to the continuous problem and with the speed $(1+\frac{1}{2}\eta_m)$ of a solitary wave of the family (1.2) with amplitude η_m.

Finally, knowing the values of η_m and x_m raises the possibility of yet another comparison, namely, the difference between the solution $\eta(t)$ of the discrete problem and the function

$$\zeta(x, t) = \eta_m \operatorname{sech}^2 \left\{ \left[\frac{3\eta_m}{4(1+\frac{1}{2}\eta_m)} \right]^{1/2} (x - x_m) \right\}. \tag{3.4}$$

The function ζ corresponds to the wave of the family (1.2) of amplitude η_m, whose crest is located at x_m. Then, analogously to the definition (3.2) we write

$$D(t) := \left\{ \sum_{i=N_1}^{N_2} [\eta(i\,\Delta x, t) - \zeta(i\,\Delta x, t)]^2 \Big/ \sum_{i=N_1}^{N_2} [\zeta(i\,\Delta x, t)]^2 \right\}^{1/2}, \tag{3.5}$$

which quantity we shall refer to as the *shape error*.

3.2. *Convergence Studies*

Since, for the convergence studies, it is sufficient to use a fixed ratio of Δx to Δt, one of our early experiments was to determine an "optimal" value for this ratio. The results of one such test (see Table I) indicate that the best accuracy was achieved when $\Delta x \simeq \Delta t$. We decided, therefore, to fix on the ratio $\Delta x = \Delta t$ $(=: \Delta)$ for the remainder of the study.

A number of convergence studies have been made using the fourth-order schemes (GEM–RK), (GEM–MS), (SN–RK) and the second-order scheme (CD–LF), the tests being carried out with solitary-wave amplitudes U of 0.1 and 1.0. A summary of the results of these experiments is given in Table II, where the errors E at times $t \simeq 30$, 70 and 120 are given. (Recall that the speed of propagation of these waves is $(1+\frac{1}{2}U)$ so that when $t = 120$ they will have travelled distances of 126 and 180 spatial units, respectively.) The rows labelled "ratio" in this table give the ratio of the numbers above and below the entry and indicate the ratio by which the error decreased when Δ was halved; for the fourth-order schemes this ratio should

TABLE I

The Errors E Obtained at $t = 19.2$ Using the (GEM–RK) Scheme for a Solitary Wave of Amplitude $U = 1.0$

	Values of Δx				
Δt	0.32	0.16	0.08	0.04	0.02
0.32	0.25(−1)	0.37(−1)	0.36(−1)	0.36(−1)	0.36(−1)
0.16	0.12(−1)	0.12(−2)	0.18(−2)	0.18(−2)	0.18(−2)
0.08	0.14(−1)	0.80(−3)	0.53(−4)	0.86(−4)	0.89(−4)
0.04	0.14(−1)	0.87(−3)	0.51(−4)	0.28(−5)	0.48(−5)
0.02	0.14(−1)	0.87(−3)	0.54(−4)	0.33(−5)	0.14(−5)

Note. These experiments had $x_0 = 11$. The numbers in parentheses indicate the exponent of 10 multiplying the preceding numbers, e.g., $0.25(-1) \equiv 0.25 \times 10^{-1}$.

approach 16 as Δ decreases to zero and should approach 4 in the same limit for the second-order scheme. That this apparently was the case for our implementations can be seen from the results with $U = 0.1$. With the larger wave amplitude, $U = 1.0$, convergence orders considerably in excess of 4 were found in many of the tests made with the fourth-order schemes, suggesting that still further mesh refinement was needed before the asymptotic convergence rate would be achieved. Under similar conditions, however, the asymptotic convergence rate was apparently realized with the second-order (CD–LF) scheme. The convergence properties of the (GEM–MS) scheme with $U = 1.0$ may seem to be somewhat anomalous, but they are probably a consequence of the fifth-order time stepping used in this scheme: with the meshes employed the dominant component of the error presumably arose from the temporal approximation and the anticipated fourth-order rates would therefore only emerge with much finer meshes or by using a different ratio for $\Delta t/\Delta x$. The run times on a CYBER 175 for the tests with $\Delta = 0.02$ were approximately 400 s (GEM–RK), 267 s (GEM–MS), and 400 s (SN–RK).

While Table II indicates the convergence properties of the schemes with Δ, the graphs in Fig. 1 indicate the temporal dependence of E for a fixed Δ. Figure 1a shows the error E for the various approximations computed with $\Delta = 0.04$ to the solitary wave having $U = 0.1$, and Fig. 1b shows the approximations found with $\Delta = 0.02$ to the wave having $U = 1.0$. (Note that E is plotted on a logarithmic scale.) The (SN–RK) scheme gave the best approximation to the smaller solitary wave whereas the (GEM–RK) scheme gave, by and large, the smallest errors for the solitary wave with $U = 1.0$. (Note that the (GEM–RK) and the (GEM–MS) schemes gave nearly the same errors for the computation of the smaller solitary wave, but for the larger wave the errors were greatly different, suggesting that the choice $\Delta t = \Delta x$ was not "optimal" for the (GEM–MS) scheme.) Both sets of graphs show an initial phase over which the error rapidly increased and after which there was a slower increase in E. Much of the slower increase arises because the

TABLE II

The Errors E Obtained When Approximating Solitary Waves of Amplitude 0.1 and 1.0

	Values of t					
	For $U=0.1$			For $U=1.0$		
Δ	30.720	72.320	120.320	30.720	72.320	120.320
0.32	0.108(−1)	0.256(−1)	0.429(−1)	—	—	—
Ratio	15.8	15.7	15.7	—	—	—
0.16	0.685(−3)	0.163(−2)	0.274(−2)	0.249(−2)	0.141(−1)	0.400(−1)
Ratio	15.9	15.8	15.9	28.4	31.3	31.3
0.08	0.430(−4)	0.103(−3)	0.172(−3)	0.876(−4)	0.451(−3)	0.128(−2)
Ratio	16.0	16.1	15.9	26.5	32.2	32.4
0.04	0.269(−5)	0.641(−5)	0.108(−4)	0.330(−5)	0.140(−4)	0.395(−4)
Ratio	—	—	—	21.4	24.4	28.8
0.02	—	—	—	0.154(−6)	0.574(−6)	0.137(−5)
			(a) (GEM–RK)			
0.32	0.107(−1)	0.255(−1)	0.429(−1)	—	—	—
Ratio	15.6	15.6	15.6	—	—	—
0.16	0.686(−3)	0.163(−2)	0.275(−2)	0.167(−1)	0.122	0.361
Ratio	15.9	15.8	15.9	13.4	15.9	16.6
0.08	0.432(−4)	0.103(−3)	0.173(−3)	0.125(−2)	0.765(−2)	0.218(−1)
Ratio	16.0	16.0	16.0	25.2	26.8	27.3
0.04	0.270(−5)	0.643(−5)	0.108(−4)	0.497(−4)	0.285(−3)	0.798(−3)
Ratio	—	—	—	27.9	29.8	30.2
0.02	—	—	—	0.178(−5)	0.956(−5)	0.264(−4)
			(b) (GEM–MS)			
0.32	0.295(−3)	0.447(−3)	0.563(−3)	—	—	—
Ratio	15.9	15.9	16.0	—	—	—
0.16	0.186(−4)	0.281(−4)	0.351(−4)	0.440(−2)	0.188(−1)	0.481(−1)
Ratio	16.0	16.0	16.0	21.4	25.1	26.9
0.08	0.116(−5)	0.176(−5)	0.219(−5)	0.206(−3)	0.750(−3)	0.179(−2)
Ratio	15.8	16.0	16.0	19.4	22.9	25.2
0.04	0.733(−7)	0.110(−6)	0.137(−6)	0.106(−4)	0.327(−4)	0.709(−4)
Ratio	—	—	—	17.2	18.8	21.2
0.02	—	—	—	0.616(−6)	0.174(−5)	0.334(−5)
			(c) (SN–RK)			
0.32	0.393(−2)	0.797(−2)	0.113(−1)	—	—	—
Ratio	3.7	3.9	4.0	—	—	—
0.16	0.106(−2)	0.203(−2)	0.283(−2)	0.143	0.311	0.496
Ratio	3.9	4.0	4.0	4.3	4.3	4.2
0.08	0.274(−3)	0.513(−3)	0.711(−3)	0.332(−1)	0.725(−1)	0.118
Ratio	4.1	4.0	4.0	4.1	4.1	4.1
0.04	0.670(−4)	0.129(−3)	0.179(−3)	0.818(−2)	0.178(−1)	0.290(−1)
Ratio	—	—	—	4.0	4.0	4.0
0.02	—	—	—	0.204(−2)	0.444(−2)	0.721(−2)
			(d) (CD–LF)			

Notes. (a) (GEM–RK) scheme; (b) (GEM–MS) scheme; (c) (SN–RK) scheme; (d) (CD–LF) scheme. $\varepsilon = 0.1 \times 10^{-7}$ for all these tests. An entry in a row labelled "ratio" is the ratio of the numbers above and below that entry.

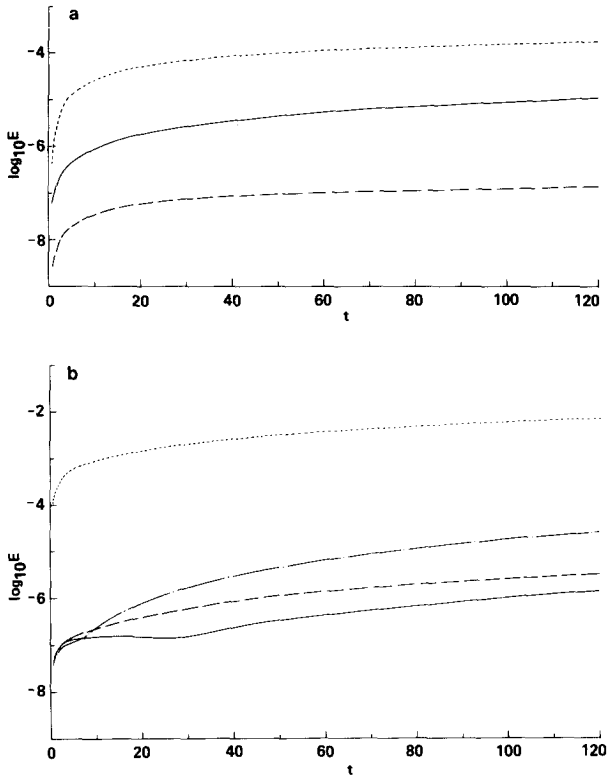

FIG. 1. The error E (plotted on a logarithmic scale) as a function of t. (a) $U = 0.1$, $\Delta = 0.04$. ——: (GEM–RK) and (GEM–MS); — — —: (SN–RK); - - -: (CD–LF). (b) $U = 1.0$, $\Delta = 0.02$. ——: (GEM–RK); - · -: (GEM–MS); — — —: (SN–RK); - - -: (CD–LF).

"amplitude" of the approximate solutions is, in general, different from that of the exact solution and therefore the two waves, having slightly different phase speeds, draw apart.

3.3. *Further Tests*

The dependence of the height error H on time for the various schemes (when $\Delta = 0.02$) is shown in Fig. 2a. The results for Fig. 2 were obtained using a solitary wave of amplitude $U = 1.0$ as the initial datum. (Note that, to normalize the errors, the ordinates in Fig. 2 have been scaled by Δ^n, where n is the order of accuracy of the scheme being used.) Thus we see that the "amplitude" of the discretely computed waveforms for both the (GEM–RK) and the (SN–RK) schemes were slightly smaller than the amplitude of the exact solution; moreover, after an initial "settling out" period, the amplitude of the approximate solution decreased monotonically

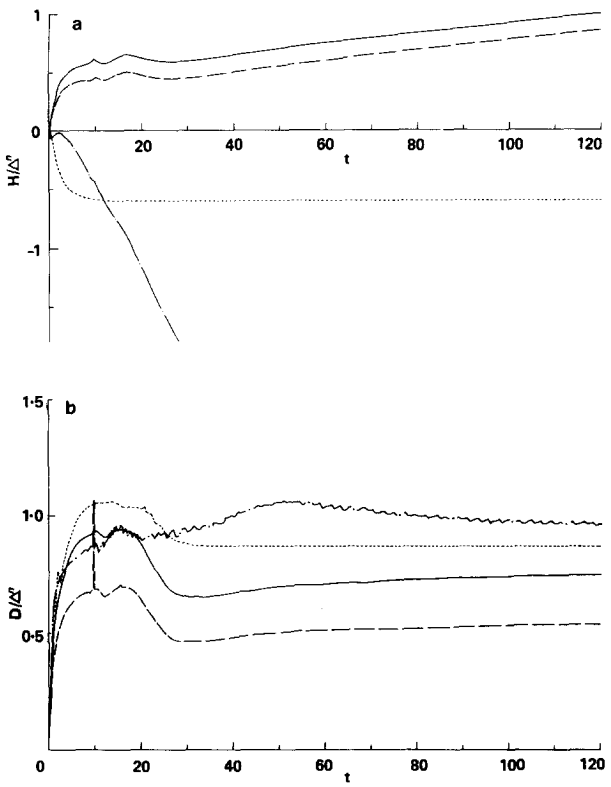

FIG. 2. Two measures of differences between approximate solutions and solitary-wave solutions, for calculations using initial data corresponding to a solitary wave of amplitude $U = 1.0$ (and $\varepsilon = 0.1 \times 10^{-7}$). ——: (GEM–RK), $n = 4$; – · –: (GEM–MS), $n = 4$; — —: (SN–RK), $n = 4$; - - -: (CD–LF), $n = 2$. These calculations had $\Delta = 0.02$. (a) $H(t)/\Delta^n$ (see 3.3); (b) $D(t)/\Delta^n$ (see 3.5).

with time. Both the (GEM–MS) and the (CD–LF) schemes, on the other hand, generated waveforms whose amplitudes exceeded that of the exact solution. Probably the most interesting feature of these computations is that the (CD–LF) scheme, in contrast to the other schemes, generated a waveform which, after an initial period, had an amplitude (or height error) independent of t. We shall consider this point in more detail below.

Another obvious feature of the graphs is the "kink" near $t = 10$. This corresponds to the time at which the crest of the wave passed the initial location of the right-hand boundary of the domain, the point where the initial datum had been truncated. This is not unexpected since the theory for problem (P) developed in [5] shows that a discontinuity of the sort generated by our truncation procedure does not propagate. (The larger errors associated with the second-order scheme presumably dominated the truncation effect so that the "blip" was not apparent in that case.)

The same effect is also apparent in connection with the "shape error" $D(t)$, shown in Fig. 2b, where a "spike" can be seen near $t = 10$ for all three of the higher-order schemes. Recall that the shape error indicates the difference between the discretely-computed waveform and a solitary wave (1.2) having the same amplitude and phase location as that of the discrete solution. Thus, the results of Fig. 2b suggest that, after an initial settling-out period of about 30 time units, the shape of the discretely-computed wave changed only rather slowly with time, with the exception of the (GEM–MS) scheme which showed some short-time variation in D superimposed on a more gradual, long term variation. In keeping with the results shown in Fig. 2a, the (CD–LF) scheme generated a waveform whose shape was eventually independent of t.

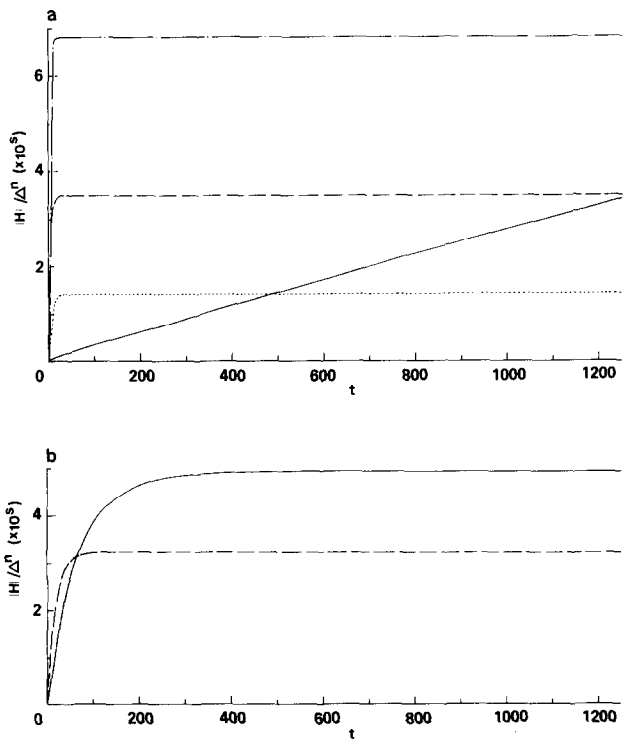

FIG. 3. The height error when $\Delta = 0.16$ for a variety of initial wave amplitudes U. ($\varepsilon = 0.1 \times 10^{-7}$.) Note the ordinates are magnified by the factor 10^s.

(a) ——: $U = 1.0$, (GEM–RK), (SN–RK), $n = 4, s = -2$, $H(1280)/\Delta^n = 34.86$;
–·–: $U = 1.0$, (CD–LF), $n = 2, s = 1$, $H(1280)/\Delta^n = -0.6722$;
— —: $U = 0.75$, (CD–LF), $n = 2, s = 1$, $H(1280)/\Delta^n = -0.3480$;
- - -: $U = 0.5$, (CD–LF), $n = 2, s = 1$ $H(1280)/\Delta^n = -0.1412$.
(b) — —: $U = 0.25$, (CD–LF), $n = 2, s = 2$, $H(1280)/\Delta^n = -0.0324$;
——: $U = 0.1$, (CD–LF), $n = 2, s = 3$, $H(1280)/\Delta^n = -0.00494$.

Thus, the above results suggest that the (CD–LF) scheme has discrete "solitary-wave" solutions, whereas none of the other schemes would appear to have this property. To provide further support for this thesis similar tests were made with a variety of different initial wave amplitudes U. This new set of experiments was made with $\Delta = 0.16$ with the calculations progressing for 8000 time steps to investigate the possibility of very slow temporal changes in H or D. The results of these tests are summarised in Figs. 3 and 4, the height errors being given in Fig. 3 and the shape errors in Fig. 4. It is seen from these graphs that the height error for the (CD–LF)

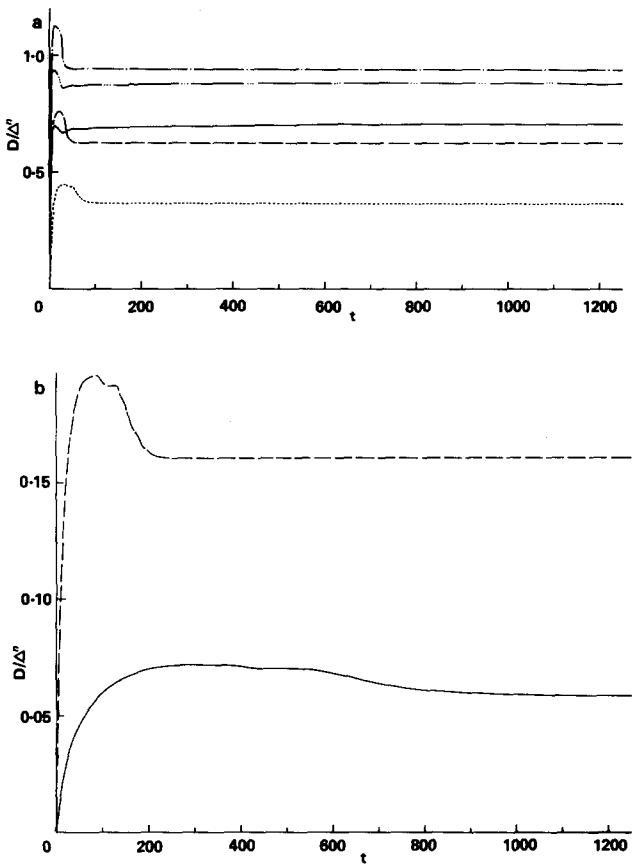

FIG. 4. The shape error when $\Delta = 0.16$ for a variety of initial wave amplitudes U. ($\varepsilon = 0.1 \times 10^{-7}$.)

(a) $-\cdots-$: $U = 1.0$, (GEM–RK), $n = 4$, $D(1280)/\Delta^n = 0.8869$;
——: $U = 1.0$, (SN–RK), $n = 4$, $D(1280)/\Delta^n = 0.7119$;
$-\cdot-$: $U = 1.0$, (CD–LF), $n = 2$, $D(1280)/\Delta^n = 0.9416$;
— —: $U = 0.75$, (CD–LF), $n = 2$, $D(1280)\Delta^n = 0.6263$;
- - -: $U = 0.5$, (CD–LF), $n = 2$, $D(1280)/\Delta^n = 0.3680$.
(b) — —: $U = 0.25$, (CD–LF), $n = 2$, $D(1280)/\Delta^n = 0.1605$;
——: $U = 0.1$ (CD–LF), $n = 2$, $D(1280)/\Delta^n = 0.05871$.

scheme quickly became constant at a value that was maintained for several thousand time steps. By contrast the height errors for both the (GEM–RK) and the (SN–RK) schemes increased steadily with time (see Fig. 3a where the case $U = 1.0$ is shown). An illustration of how nearly constant the height error was for the (CD–LF) scheme is as follows. At $t = 23.04$, $H = -0.01746$ (rounded to 4 significant digits) and from then until $t = 1280.00$ the height error was either -0.01746 or -0.01747, with the fluctuation in the fourth digit probably arising as a consequence of the height-locating procedure that was used (cf. Section 3.1). The times taken for the steady situation to be attained were found to depend rather strongly on the amplitude U of the initial datum, a feature that is evident in Fig. 3, but which appears more obviously in the graphs of the shape error shown in Fig. 4. Thus, when $U = 1.0$ it took only about 40 time units for the steady waveform to be realized whereas with $U = 0.1$ it took at least 1000 time units for the discrete waveform to reach its steady value. (It is interesting that Ablowitz and Ladik [2], and see also Hirota [15], have discovered a numerical scheme for the Korteweg–de Vries equation (1.1) that has exact soliton solutions. This scheme is not local in space, however, and it is not known whether there are local schemes for (1.1) having exact travelling-wave solutions.)

Also given in Fig. 4a are graphs of the shape error D for both the (GEM–RK) and the (SN–RK) schemes, for the case $U = 1.0$. It can be seen from these graphs that the variations of D with time were quite small when t exceeded about 100. Note that this does not mean the discrete wave nearly has permanent form for, as we saw in Fig. 3, the "amplitudes" of these discrete solutions decreased steadily with time. Rather, the interpretation is that, for $t > 100$ say, the "shape" of these discrete solutions differed from a solitary wave (1.2) of the same amplitude by approximately a constant proportion. Thus, although the amplitudes of these approximations to the solitary wave (1.2) decreased steadily with time the waveform preserved a shape close to that of a member of the family (1.2).

Some of the values of D/Δ^4 for the (GEM–RK) scheme, from which the graph in Fig. 4a was drawn are given in Table III.

TABLE III

Some Values of D/Δ^4 for the (GEM–RK) Scheme, $U = 1.0$, $\varepsilon = 0.1 \times 10^{-7}$, $\Delta = 0.16$, Corresponding to the Graph Shown in Fig. 4a.

t	99.84	199.68	299.52	399.36	499.20	599.04	701.44
D/Δ^4	0.8777	0.8812	0.8825	0.8838	0.8865	0.8860	0.8855
t	801.28	901.12	1000.96	1100.80	1200.64		
D/Δ^4	0.8841	0.8850	0.8829	0.8835	0.8795		

4. Conclusions

A description has been given of a number of numerical schemes to solve the initial-value problem (P). The methods studied have either second- or fourth-order accuracy in both the space and time variables, though one of the schemes has a straightforward extension to any desired order of accuracy. Rigorous error estimates can be obtained for all these schemes using the methods described in [9]. A description is also given of some numerical experiments made with these schemes based on the solitary-wave solution (1.2) of (P). The experiments, which included both a standard convergence study and other special tests, revealed some subtle differences between the errors for the various schemes. So, for example, the multi-step scheme appeared to introduce an oscillatory component to the solution, as indicated by the shape error D (cf. Fig. 2), whereas the others apparently did not. On the other hand, the (CD–LF) computations appeared to settle into a permanent-form solution of its own, a property not evident with the other schemes.

In purely practical terms we found the convergence study invaluable, by way of exposing errors both in the programming and of a conceptual kind, and as a guide to performing the computations described in Bona, Pritchard, and Scott [8–10].

Finally, the numerical evidence that the (CD–LF) scheme might have permanent-form (solitary-wave) solutions was a surprise to us and it would be of interest to know definitively whether or not this is the case. (We have not as yet attempted to find an explicit solitary-wave solution to the present problem, or to demonstrate the existence of such by an abstract argument.) Should a family of such solutions exist it would be interesting to enquire whether or not they would exhibit the so-called soliton property, namely, that two solitary waves of the family would reemerge from an interaction with their shapes unaltered. We believe the answer to this question to be in the negative for the following reason. If the (CD–LF) scheme were to have the soliton property for all Δt and Δx, then the convergence estimates referred to in Section 2 would imply that the same holds for (P): as Δt and Δx tend to zero, the solitary-wave solutions to (CD–LF) would converge to a solitary-wave solution of (P). But the numerical experiments described in [1] and [8] indicate that (P) does *not* have the soliton property. (Inelastic collisions of two solitary waves having positive and negative amplitudes, respectively, have been reported in [11] and [18].) It should, however, be stressed that the above argument is not a proof, even given the existence of (CD–LF) solitary waves.

Acknowledgments

This work was partially supported by the following contracts: Brookhaven National Laboratory, Contract EY-36-C-02-0016; ICASE at NASA Langley, contract NAS1-14101; Air Force Contract F49620-79-C0149; Mathematics Research Center, Madison, Contract DAAG29-80-C-0041; The National Science Foundation. The authors thank Chris Eilbeck and another referee for helpful remarks.

REFERENCES

1. KH. O. ABDULLOEV, I. L. BOGOLUBSKY, AND V. G. MAKHANKOV, *Phys. Lett. A* **56** (1976), 427–428.
2. M. T. ABLOWITZ, AND J. F. LADIK, *J. Math. Phys.* **17** (1976), 1011–1018.
3. M. E. ALEXANDER AND J. L. MORRIS, *J. Comput. Phys.* **30** (1979), 428–451.
4. D. N. ARNOLD, J. DOUGLAS, AND V. THOMÉE, *Math. Comp.* **36**, No. 153 (1981), 53–63.
5. T. B. BENJAMIN, J. L. BONA, AND J. J. MAHONY, *Philos. Trans. Roy. Soc. London A* **272** (1972), 47–78.
6. J. L. BONA, AND P. J. BRYANT, *Proc. Cambridge Philos. Soc.* **73** (1973), 391–405.
7. J. L. BONA, AND V. A. DOUGALIS, *J. Math. Anal. Appl.* **75** (1980), 503–522.
8. J. L. BONA, W. G. PRITCHARD, AND L. R. SCOTT, *Phys. Fluids* **23** (1980), 438–441.
9. J. L. BONA, W. G. PRITCHARD, AND L. R. SCOTT, *Philos. Trans. Roy. Soc. London A* **302** (1981), 457–510.
10. J. L. BONA, W. G. PRITCHARD, AND L. R. SCOTT, *in* "Proceedings of the AMS–SIAM Conference on Fluid Dynamical Problems in Astrophysics and Geophysics" (N. R. Lebovitz, Ed.), Lectures in Appl. Math. Vol. 20, pp. 235–267, Amer. Math. Soc., Providence, R. I., 1983.
11. J. COURTENAY LEWIS, AND J. A. TJON, *Phys. Lett. A* **73**, 275–279.
12. J. C. EILBECK AND G. R. MCGUIRE, *J. Comput. Phys.* **19** (1975), 43–57.
13. J. C. EILBECK, AND G. R. MCGUIRE, *J. Comput. Phys.* **23** (1977), 63–73.
14. H. A. GOLDSTINE, "A History of Numerical Analysis from the 16th Through the 19th Century," Springer-Verlag, New York, 1977.
15. R. HIROTA, *J. Phys. Soc. Japan* **43** (1977), 1424–1433.
16. J. D. LAMBERT, "Computational Methods in Ordinary Differential Equations," Wiley, London, 1973.
17. D. H. PEREGRINE, *J. Fluid Mech.* **25** (1966), 321–330.
18. A. R. SANTARELLI, *Nuovo Cimento B* **46** (1978), 179–188.
19. R. E. SHOWALTER, *Appl. Anal.* 7 (1978), 297–308.
20. J. STOER, AND R. BULIRSCH, "Introduction to Numerical Analysis," Springer-Verlag, New York, 1979.
21. L. WAHLBIN, *Numer. Math.* **23** (1975), 289–303.